ЕРЕВАНСКИЙ ФИЗИЧЕСКИЙ ИНСТИТУТ

ЕФИ 230 (23)-77

S.G. GRIGORYAN, S.B. YESAYBEGYAN,
N.L. TER-ISAAKYAN

THE BEHAVIOUR OF THE HADRONIC STRUCTURE FUNCTIONS AT $X \to 1$

ЕРЕВАН 1977 ЕРЕВАН

YERSVAN PHYSICS INSTITUTE

ЕФИ 230 (23)-77

S.G.GRIGORYAN, S.B.YESAYBEGYAN, N.L.TER-ISAAKYAN

ON THE BEHAVIOUR OF THE HADRONIC STRUCTURE FUNCTIONS AT $X \to 1$

Yerevan 1977

1. Introduction

The idea that hadrons can be considered as bound states of quarks results in some interesting predictions confirmed in experiments. The counting rules for elastic [1] and inelastic [2] large angle scattering processes have been derived in some papers. These counting rules define the asymptotic cross sections behaviour at large momentum transfer q^2. Their derivation is based on the assumption that the quarks binding energy can be neglected at large q^2 and the interaction of free quarks defines the hadronic process amplitude.

The success of the additive quark model in description of the static properties of hadrons [3] as well as differential and total cross sections at high energies apparently means that the quarks in hadron are bound weakly.

The model of strong interaction based on the colored quarks interaction with the octet of colored vector gluons is asymptotically free. That seems to correspond to the picture,

given above. Such a model makes it possible to obtain predictions more detailed than in [1-2]. The interesting polarization properties of electroproduction structure functions have been derived by G.Farrar and D.Jackson [6] for $X \to 1$. The decay of charmonium has been dealt with in a number of papers and a lot of experimentally confirmed predictions has been obtained (see e.g.Ref. [7]).

In this work we investigate the behaviour of the structure functions for the n-quark bound state, in the limit when one of the quarks carries nearly all the momentum of the incoming particles $(X \to 1)$.

Our results can be used to determine the probability of finding "nonvalence" quark in the hadron in the assumption that one can find many quark bound states in the physical baryon and meson. These results can be also applied to the light nuclei which can be considered at large momentum transfer as consisting of correspondent number of quarks.

For the octet of baryons the relations between structure functions are obtained, the differences of strange and nonstrange quarks masses accounting for the SU(3)- symmetry breaking. The average transverse momentum of the quark with $X \to 1$ is estimated as well.

We start from the same assumptions made in Ref. [1-2, 6]. The mesons and baryons are s-wave bound states of quark-antiquark and three quarks, respectively. In the "normal" wave function the quarks carry the finite fraction of the incoming momentum, their transverse momenta being restricted. The "exeptional" wave

function (one quark carrying nearly all the momentum of incoming particle) can be generated from the "normal" wave function by means of free quark interaction diagrams, of which those corresponding to the lowest order perturbation theory are shown in Fig.1. Each propagator in these graphs has a large invariant mass $\left(\sim \frac{m_\perp^2}{1-x}\,,\ m_\perp^2 \approx \kappa_\perp^2 + m^2\right)$ when $x \to 1$. Hence, the application of perturbation theory is justified. For our consideration we use the time-ordered perturbation theory utilizing the properties of vertices and propagators in the region, we are interested in: $1 \gg 1-x \gg \frac{m^2}{Q^2}$, $Q^2 \to \infty$.

In such a way it seems easier to single out the leading terms and to investigate the properties of structure functions.

2. Kinematics and Properties of Vertices

Let us consider, for example, the diagram of Fig.1a. The notation is clear from the figure. In the centre of mass frame we use the following parametrisations for incoming and outgoing momenta of quarks

$$\begin{aligned} \vec{p}_i &= z_i \vec{P} + \vec{p}_{i\perp} \quad ; \quad \vec{p}_{i\perp}\vec{P} = 0 \\ \vec{p}_i' &= x_i \vec{P} + \vec{k}_{i\perp} \quad ; \quad \vec{k}_{i\perp}\vec{P} = 0 \end{aligned} \tag{1}$$

The momentum of incoming hadron $\vec{P}$ has been chosen along the z-axis. We have the following kinematical relations up to the terms of order $\frac{m^2}{Q^2}$:

$$-q^2 = Q^2 = 4\vec{P}^2 x(1-x)$$

$$\chi|\vec{q}| = \sqrt{Q^2/x(1-x)}$$
$$q_0 = |\vec{q}|(1-2x) \qquad (2)$$

where $\chi = -\frac{q^2}{2Pq}$. The momenta of of the outgoing quarks are low in the limit $\chi \to 1$ due to momentum conservation: $x_2 + x_3 = 1 - \chi$. The four momenta squares of virtual particles are large:

$$-\kappa_1^2 = (x_2 + x_3)\left(\frac{m_{2\perp}^2}{x_2} + \frac{m_{3\perp}^2}{x_3}\right)$$
$$m_1^2 - p_1^2 = \frac{m_{2\perp}^2}{x_2} + \frac{m_{3\perp}^2}{x_3} \qquad (3)$$
$$-\kappa_2^2 = \frac{z_3}{x_3}\, m_{3\perp}^2$$
$$m_2^2 - p_{f1}^2 = z_3\left(\frac{m_{3\perp}^2}{x_3} + \frac{m_{2\perp}^2}{x_2}\right)$$

In the formula (3) and in what follows the terms of order $\frac{m^2}{Q^2}$ and $(1-\chi)$ are neglected.

Let us consider the vertex of gluon emission by quarks $\Phi_1^{S_2 S_1}(\lambda) = \bar{u}^{S_2}(p_2)\, \hat{e}^{*}(\lambda)\, u^{S_1}(p_1)$, the quarks being off shell where S_2 and S_1 helicities of the outgoing and incoming quarks, respectively; e_μ^λ is the gluon polarisation vector. We don't use the colour indices, since they are not important for our calculation . For the transverse gluon we find:

$$\Phi_1^{S,S}(\lambda) = -i\sqrt{2\varepsilon_1\varepsilon_2}\left\{(\lambda+2S)\left[\sin\frac{\theta_2}{2}\cdot e^{i(2\varphi-\varphi_1-\varphi_2)S} - \frac{\sin\theta}{2}\, e^{i(\varphi_2-\varphi_1)S}\right]+\right.$$
$$\left.(\lambda-2S)\left[\sin\frac{\theta_2}{2}\cdot e^{-i(2\varphi-\varphi_1-\varphi_2)} - \frac{\sin\theta}{2}\cdot e^{i(\varphi_2-\varphi_1)S}\right]\right\} \qquad (4)$$

$$\Phi_1^{S,-S}(\lambda) = -\frac{m(\varepsilon_1-\varepsilon_2)}{\sqrt{2\varepsilon_1\varepsilon_2}}\,(\lambda-2S)\, e^{i\frac{\pi}{4}(\lambda-2S)}\, e^{-i(2\varphi-\varphi_1-\varphi_2)S} \qquad (5)$$

For the longitudinal gluon the current's zero component can be derived from the third component.

As a result, after summing over virtual gluon polarizations we have to multiply the third component by $\sqrt{\frac{-K^2}{K_0^2}}$ (where K is virtual gluon 4-momentum) to obtain the effective longitudinal gluon contribution:

$$f_1^{SS}(3) = -2i\sqrt{\varepsilon_1\varepsilon_2}\cdot\sqrt{-\frac{K^2}{K_0^2}}\; e^{i(\varphi_2-\varphi_1)S} \qquad (6)$$

$$f_1^{S,-S}(3) = -2iS\sqrt{-\frac{K^2}{K_0^2}}\cdot\frac{m(\varepsilon_1-\varepsilon_2)}{\sqrt{\varepsilon_1\varepsilon_2}}\left[\sin\frac{\theta_1}{2}\, e^{i(\varphi_2-\varphi_1)S} + \sin\frac{\theta_2}{2}\, e^{i(\varphi_1-\varphi_2)S}\right] \qquad (7)$$

where θ,φ ; θ_1,φ_1; θ_2,φ_2 are the polar and azimuthal angles of vectors $\vec{K}$, $\vec{P}_1$ and $\vec{P}_2$ respectively: $\varepsilon_i=\sqrt{\rho_i^2+m_i^2}$ is noncovariant energy of the quark which is, generally speaking, different from the zero-component of four vecto. P_{i0} In the formulae (4-7) high powers of sines are neglected. With an accuracy up to unessential phase factor, the annihilation vertices of the type of $f_2^{S_2,S_1}(\lambda) = \bar{u}^{S_2}(P_2)\,\hat{e}^{*}(\lambda)\,v^{-S_1}(P_1)$ and $f_3^{S_2S_1} = \bar{v}^{-S_2}(P_2)\,\hat{e}^{*}(\lambda)\,u^{S_1}(P_1)$ can be derived from formulae (4-7) by replacing $\varepsilon_1\to-\varepsilon_1$; $S_1\to-S_1$ and $\varepsilon_2\to-\varepsilon_2$; $S_2\to-S_2$ respectively.

If the virtual gluon is absorbed in the vertex one has to replace in all the formulas $\lambda\to-\lambda$

One can easily see that the diagrams of the type shown in Fig.1 dominates in the limit $Q^2\to\infty$ ($x\to1$). In such diagrams the momentum is transfered from left to right and from the lowest quark up to the higheet one, when the highest quark is struck by virtual photon and the time axis is directed from

left to right. Other types of diagrams are suppressed. In the diagram of Fig.1b, for instance, $\vec{P}_{f_2} = -\vec{P}_3$ and the corresponding propagator

$$\frac{1}{\varepsilon_2 - \varepsilon_{K_2} - \varepsilon_{f_2}} \cdot \frac{1}{2\varepsilon_{f_2}} \sim \frac{1}{\vec{P}^2}$$

is small as compared to the corresponding propagator in the Fig. 1a where $\vec{P}_{f_2} = \vec{P}_3$

$$\frac{1}{2\varepsilon_{f_2}} \cdot \frac{1}{\varepsilon_3 - \varepsilon_{f_2} - \varepsilon_2' - \varepsilon_3'} \approx \frac{1}{P_{f_2}^2 - m^2} \sim \frac{m^2}{1-x} \qquad (9)$$

It isn't difficult to note that the energy denominators of noncovariant theory (multiplied by $\frac{1}{2\varepsilon}$) are reduced to those of covariant theory as in the case of formula (9). Therefore, for the analysis of propagator contributions in the diagrams it is sufficient to use the formula (3). When the momentum of one of the quarks in the vertex is small (as it is in the lowest vertex in Fig 1a), the first term only remains in the formula (4) in the limit $x \to 1$ ($P_2 \sim x_2 P \sim (1-x)P$). As a result, the vertices for transverse gluon in that case behave like $\frac{1}{\sqrt{1-x}}$. Such vertices will be called "good".

$$f_L^{s,s}(\lambda) = -ip_{21}\sqrt{\frac{\varepsilon_1}{2\varepsilon_2}}(\lambda+2s)\, e^{i(2\varphi-\varphi_1-\varphi_2)s}$$

$$f_1^{-s,s}(\lambda) = -im\sqrt{\frac{\varepsilon_1}{2\varepsilon_2}}(\lambda+2s)\, e^{i(2\varphi-\varphi_1-\varphi_2)s}\, e^{i\frac{\pi}{4}(\lambda+2s)} \qquad (10)$$

In these vertices the gluon and fast quark have aligned helicities. The vertices with any other configuration of helicities are suppressed by the factor (1-x) at least (the third and fourth term in the formula (4)). The average transverse moments of outgoing quarks are of order of quark masses

and, therefore $f_1^{SS}(\lambda) \sim f_1^{S,-S}(\lambda)$ . . For the longitudinal gluon, as it is seen from formulas (3), (7), (6) the vertex $f_1^{S,-S}(\lambda)$ are suppressed in the limit $Q^2 \to \infty$ and the vertex $f_1^{SS}(3)$ is "bad" when $\chi \to 1$, i.e. $f_1^{SS}(3) \sim m$.

If the momenta of two quarks in the vertex are large $p_1 \sim p_2 \sim p$ the vertex is "bad" for transverse gluon. For longitudinal gluon the vertex $f_1^{SS}(3)$ is "good".

The properties of annihilation verteces are analogous. As a result of the properties of vertices the diagram of Fig. 1a dominates in the limit $\chi \to 1$ for $n = 3$, the lowest gluon being transverse and the highest one being longitudinal. The two lower quarks have antialigned helicities and hence the quark which is struck by virtual photon must have the same helicity as the incoming hadron. Other diagrams are suppressed by the factor $(1-\chi)$ at least. For instance, there are two "bad" vertices in the diagram of Fig. 1b.

The quark-quark-virtual photon vertex can be also obtained from the formula (4) in which $\sin^{\theta_{12}}/_2 \sim 1$ should be set, since when one integrates over outgoing quark momenta, the main contribution comes from the region in which the vectors $\vec{p}_1$ and $\vec{p}$ are antiligned. This vertex are of the order of $\sqrt{Q^2}$ for transverse photon and of the order of m for longitudinal photon.

3. General Case of n-Quark Bound State

Let us consider the n-quarks S-wave bound state.

When $n \leq 3$ the diagrams with 3 - gluon vertex do not contribute, since the incoming particle is uncolored. For $n>3$ the digrams with 3 - and 4 - gluon vertices can contribute. At first we shall restrict ourselves to Abelian case where there are no such vertices. Let n be odd. Utilizing the properties of vertices, one can easily see that the diagrams of the type shown in Fig.2 dominates when $x \to 1$, the transverse and longitudinal gluons being alternated from bottom to top. The contribution of each vertex to the amplitude is of order $\frac{1}{\sqrt{1-x}}$ and the propagator contribution is of order $1-x$. Integrating over the phase space of the outgoing quarks we obtain for the transverse part of the structure function:

$$F_\perp(x) \sim (1-x)^{2n-3}, \qquad (11)$$

The longitudinal part of structure function is suppressed by a factor $\frac{m^2}{Q^2}$ relative to (11). The helicities of the quarks exchanging transverse gluon are opposite and therefore the incoming particle must have the same helicity as the highest quark. For the helicity of incoming particle $|\lambda| \neq \frac{1}{2}$ the structure is suppressed by a factor

$$(1-x)^{2|\lambda|-1} \qquad (12)$$

relative to (11).

For even n the diagrams of the type shown in Fig. 3 dominate. There is only one "bad" vertex in such diagrams which may be occur in the lower part (Fig.3a), in the intermediate part (Fig.3b) or in the upper part of the diagram (Fig.3c). For the transverse part of the structure function we obtain:

$$F_\perp(x) \sim (1-x)^{2n-2} \tag{13}$$

The helicities of the $n-2$ quarks must be opposite hence the structure functions are suppressed by the factor

$$(1-x)^{2|\lambda|-2} \tag{14}$$

relative to (13) when the helicity of incoming particle $\lambda \gg 2$

For the longitudinal photon the structure functions vanish in the scaling limit, however for even n in the region $\frac{m^2}{Q^2} \ll 1-x \sim \sqrt{\frac{m^2}{Q^2}}$ they are of the same order as in the case of transverse photon. The diagram of Fig.4 dominates in that case. All vertices and propagators except the two upper ones in this diagram behave like $\frac{m}{\sqrt{1-x}}$ and $\frac{1-x}{m^2}$ respectively when $x \to 1$. The two upper vertices behave like $\sqrt{Q^2}\sin\frac{\theta_1}{2}$ and $\sqrt{Q^2}\sin\frac{\theta_2}{2}$ because of $(-p_0^2) \sim Q^2$ and $(-K^2) \sim Q^2 \sin^2\frac{\theta_1}{2}$. The analysis of the arising integrals shows that the main contribution in the region of our interest comes from the angles θ_1 and θ_2 of order of one. Hence, the contributions of gluon propagator and vertices in the upper part compensate each other. In that case the vertex with longitudinal photon is of order $\sqrt{Q^2}$ and for the structure function we have

$$F_L(x) \sim \frac{m^2}{Q^2}(1-x)^{2n-4} \tag{15}$$

In this case all the helicities of the incoming quarks are opposite in pairs otherwise the structure function is suppressed by

$$(1-x)^{2|\lambda|} \tag{16}$$

where λ is the helicity of the incoming particle.

In the non-Abelian case the 3-gluon and 4-gluon diagrams may give contribution. The corresponding Feynman rules may be found for instance in Ref. [9].

In the limit we are interested in the 3-gluon vertex $f_{\lambda_1\lambda_2\lambda_3}(K_1,K_2,K_3)$ possesses the following properties:

$$f_{\lambda_1\lambda_2\lambda_3} \sim K_\perp \qquad \begin{cases} \lambda_i = \pm 1 \\ \lambda_1 - \lambda_2 - \lambda_3 = \pm 1 \end{cases} \tag{17}$$

$$\begin{cases} f_{0,\lambda_2,-\lambda} \sim \sqrt{K_1^2} \sim \dfrac{m}{\sqrt{1-x}} \\ f_{\lambda_1,-\lambda_2,0} \sim \sqrt{-K_3^2} \sim \dfrac{m}{\sqrt{1-x}} \end{cases} \qquad \lambda = \pm 1 \tag{18}$$

(λ_i: helicities of quarks; K_1: incoming momentum; K_2 and K_3 outcoming momenta); $K_\perp \sim m$ is a magnitude of order of gluon average transverse momentum. The 3-gluon vertex with any other configurations of helicities is suppressed by factor of order $\frac{K_\perp}{P}$.

For odd n the digrams with 3-gluon vertices can be obtained from the diagrams of Fig.2 by means of replacements shown in Fig. 5a and Fig.5b. The dependence of the amplitude on x and the helicity relations remain the same after such replacements, as it follows from the properties of 3-gluon vertex. As a result of such replacements blocks arise in which two or more gluons turn into one gluon, the helicities of incoming gluons being antialigned (Fig.6). The diagrams with 4-gluon vertices can be obtained by means of replacements in the blocks of Fig.6, as it is shown in Fig.7. The 4-gluon vertex behaves like a constant in the limit $Q^2 \to \infty$, $x \to 1$ if all the gluons are transverse and the helicity in the vertex is conserved. For any other configuration of helicities the four-gluon

vertex is suppressed. Therefore, as a result of the replacements of Fig.7a, the behaviour of the diagrams isn't changed, while the replacements of Fig.7b lead to suppressed diagrams.

For even n the replacements in the blocks with "bad" vertices are also necessary. One can easily see that in this case also all the results of the Abelian theory are valid. The cases $n=2$ and $n=3$ for π-meson and proton has been considered by G.Ferrar and D.Jackson[6]. For vector mesons we have obtained additional polarization relation for the longitudinal part of structure function. It follows from (15) and (16):

$$F_4^{\lambda} \simeq \frac{m^2}{Q^2}(1-x)^{2|\lambda|} \qquad (19)$$

The probability of finding the "nonvalence" quark in meson and baryon corresponds to the cases $n=4$ and $n=5$. For baryon we have $F_1(x) \sim (1-x)^7$ in agreement with existing parametrisations see, e.g.Ref.[10]). The helicity of the "nonvalence" quark struck by virtual photon should be, to leading order, the same as that of the baryon. For mesons the structure function corresponding to virtual photon with "nonvalence" quark behaves like $(1-x)^6$ in contrast to $(1-x)^5$ parametrisation of Ref.[10]

If the helicity of incoming meson is equal to zero, the probability of longitudinal photon interaction with nonvalence quark is of the same order as that for the transverse photon: $F_4^{\lambda=0} \sim (1-x)^4 \frac{m^2}{Q^2}$ in the region $(1-x)^2 \sim \frac{m^2}{Q^2}$. For the helicity of vector meson $\lambda \neq 0$ the structure function is suppressed: $F_L^{\lambda=\pm 1} \sim (1-x)^6 \frac{m^2}{Q^2}$

For even n the Drell-Yang-West relation[11]

$$F(x)\Big|_{x\sim 1-m^2/Q^2} \sim Q^2\left|F(Q^2)\right|^2 \qquad (20)$$

isn't valid for the scaling part of structure function, if counting rules [1] are used for the form-factor $F(Q^2)$.

However the relation (20) will be valid if one takes into account the nonscaling part of the structure function (15).

4. Relations Among Structure Functions of Baryons

The dependence of the structure functions on X and polarisation relations in the limit $X \to 1$ have been obtained above with the only assumption that incoming quarks carry the finite fraction of incoming momentum and their transverse momenta are restricted.

Let us now estimate the dependence of baryon structure functions on quark masses. In addition we assume that the quarks can be considered as nonrelativistic and in the first approximation the binding energy can be neglected. Such an assumption seems to be quite reasonable in the light of additive quark models.

The diagram of Fig.1a apparently dominates when $X \to 1$. We parametrize the four-momenta of incoming quarks in the form: $P_\mu^i = z_i P_\mu$, $z_i = \frac{m_i}{M}$ where M is the baryon mass. One can write the baryon-three-quark vertex in the form

$$\psi(p_1,p_2)\left[\bar{u}(p_1)\,u(p)\right]\left[\bar{u}(p_2)\gamma_5 C\,\bar{\tilde{u}}(p_3)\right] \qquad (21)$$

where $C=\gamma_2\gamma_4$ is the charge conjugation matrix.

The energy denominators which correspond to propagators of

incoming quarks in Fig.1a are included in the vertex function $\psi(P_1 P_2)$. This formula has to be symmetrized according to the SU(6) structure of wave function. (see for instance the table in Ref.[13]). After integrations over P_1 and P_2 the contribution of diagram of Fig. 1a is defined by that of the corresponding free quark diagram multiplied by $\psi(0) = \int \psi(P_1, P_2)\, d^4P_1 d^4P_2$ In the limit of zero binding energy for the product of spinors in (21) one has

$$|(\bar{u}(P_1)u(p))\cdot(\bar{u}(P_2)\gamma_5 C\,\bar{\tilde{u}}(P_3))|^2 \sim m_1 m_2 m_3 M$$

For the differential probability of finding a quark with mass m_1 in a baryon consisting of quarks with masses m_1, m_2, m_3 we obtain:

$$\frac{dF(x)}{dx_2\, dm_{2\perp}^2\, dm_{3\perp}^2} \simeq A_0\,\psi(0)\,\frac{z_1^2 z_2^2 z_3^2}{(z_2+z_3)^2}\cdot\frac{x_2^2 x_3^2 m_{2\perp}^2 m_{3\perp}^2}{[m_{2\perp}^2 x_3 + m_{3\perp}^2 x_2]^4}\times \tag{22}$$

$$\times\left(\frac{x_2}{z_2 m_{2\perp}^2}+\frac{x_3}{z_3 m_{3\perp}^2}\right)^2$$

The magnitude $\psi(0)$ is assumed universal for the baryon octet. The coefficient A_0 appears because of the $SU(6)$ symmetry breaking by gluon exchanges (the helicities of the lower two quarks on Fig. 1a are antialigned). Integrating over $m_{3\perp}^2$, $m_{2\perp}^2$ and x_2 we obtain the total probability of finding a quark with a mass m_1 when $x \to 1$:

$$F(x) \simeq A_0 \frac{M^4}{(m_2+m_3)^4}\,\frac{m_1^2}{m_2^2}\,f(d)\,(1-x)^3 \tag{23}$$

$$f(d) = \frac{\ln d^2}{(d^2-1)^3}\left[1+3d^2+d^4+\frac{2d^2(1+d^2)}{(1+d)^2}\right] - \frac{1}{(d^2-1)^2}\left[\frac{5(1+d^2)}{2}+\frac{1+10d^2+d^4}{3(1+d)^2}\right]$$

where $d = \frac{m_3}{m_2}$. If $m_2 = m_3$ $f(d) = 1/6$. The ratio of the masses of strange and nonstrange quarks is assumed to be $m_s/m_u \simeq 1.5$.

The results for baryon octet are summarized in the Table, where the $F_{B_i}^{q_i}$ is the ratio of the probability of finding a quark q_i in a baryon B_i to that of finding a down quark in the proton. In the first column the values of $F_{B_i}^{q_i}$ are given in the exact SU(6)symmetry, in the second column $F_{B_i}^{q_i}$ are given in the case when spin symmetry is broken due to gluon exchanges (that is the relative values of coefficient A_{ik}), and in the third column quarks mass differences are taken into account as well.

For the Λ- and Ξ- hyperons these two symmetry breaking effects work coherently and the contribution of the strange quark dominates when $x \to 1$. For the Λ - hyperon such an effect has been assumed in Ref. [14] under quite different arguments. For the Σ- hyperons these symmetry breaking effects are opposite and the probabilities of finding strange and nonstrange quarks are of the same order.

Using (22) we can define the average transverse momentum of the quark with $x \to 1$. For $m_1 = m_3$ we find: $\langle p_\perp^2 \rangle = 6 m_2^2$ for $m_3/m_2 = 1.5$ $\langle p_\perp^2 \rangle = 18\, m_2^2$

Our estimation differs from that of P.V.Landanoff [15]. In that paper it is supposed, that the invariant mass of the remained system of the quarks when one of the quark is struck by virtual photon is of the order of 2 GeV. Here for the invariant mass of second and third quarks we have $W^2 \simeq 12 m_2^2 \sim 1.1$ Gev for $m_1 \simeq m_3$, $x \to 1$.

The results obtained are valid for the e^+e^- - annihilation structure functions as well, because the corresponding

quark diagrams differ from those studied above by the substitution of outgoing quarks by antiquarks.

The strange quark dominance near $x = 1$ must result in strong correlations in the processes e^+e^- - annihilation when two fast particles are dedected in two opposite directions. If a fast Λ hyperon is dedected, we should expect a large yield of fast K^+, K^0 mesons in the opposite direction, whereas the π and $\bar{K}$ meson yield must be suppressed. For the Σ hyperon these effects must be much less and for proton and neutron yield of the strange particles in the opposite direction has to be suppressed.

The results obtained allow to predict numerically the magnitude of the polarisation effect due to weak neutral currents in the inclusive baryon production for $x \to 1$ [16]. In particular, the strong suppression of u and d - quark contribution into the Λ-hyperon results in the fact that the Λ hyperon helicity reaches 30%, while for the Σ^+ hyperon this magnitude is 15%.

The authors are grateful to S.G.Matinyan for helpful comments and discussions. We also wish to thank I.A.Azmauryan, G.G.Grigoryan, O.V.Kancheli, A.M.Kotsinyan and A.G.Sedrakyan for useful discussions.

able. The relative probabilities of finding the quark q_i in the baryon B_i : $F_{B_i}^{q_i}$

$F_{B_i}^{q_i}$	The exact SU(6)	The exact SU(3)	SU(6) broken; different quark masses
$F_p^d = F_n^u$	I	I	I
$F_p^u = F_n^d$	2	5	5
$F_{\Sigma_o}^u = F_{\Sigma_o}^d$	I	2.5	I.32
$F_{\Sigma_o}^s$	I	I	4.I7
$F_\Lambda^u = F_\Lambda^d$	I	I.5	0.79
F_Λ^s	I	3	I2.5
$F_{\Xi^o}^u = F_{\Xi^-}^d$	I	I	0.28
$F_{\Xi^o}^s = F_{\Xi^-}^s$	2	5	I0.I
$F_{\Sigma^+}^u = F_{\Sigma^-}^d$	2	5	2.64

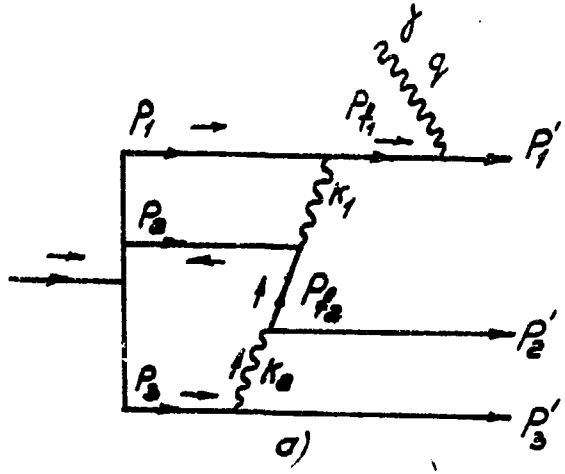
γ
q
P_1
P_{f_1}
P_1'
P_2
K_1
P_{f_2}
P_2'
P_3
K_2
P_3'

а)

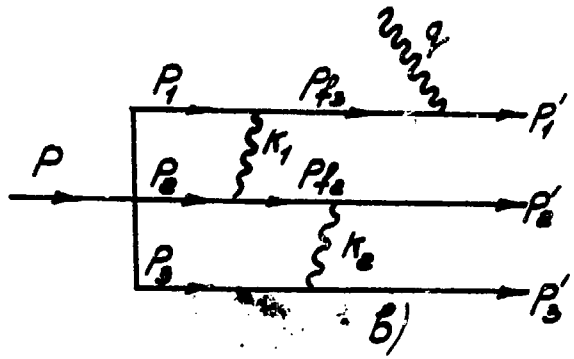
q
P_1
P_{f_3}
P_1'
P
K_1
P_2
P_{f_2}
P_2'
K_2
P_3
P_3'

б)

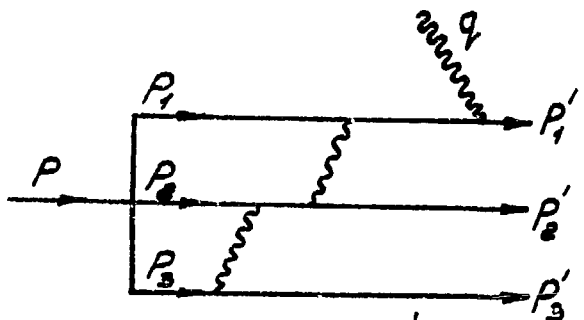
q
P_1
P_1'
P
P_2
P_2'
P_3
P_3'

с)

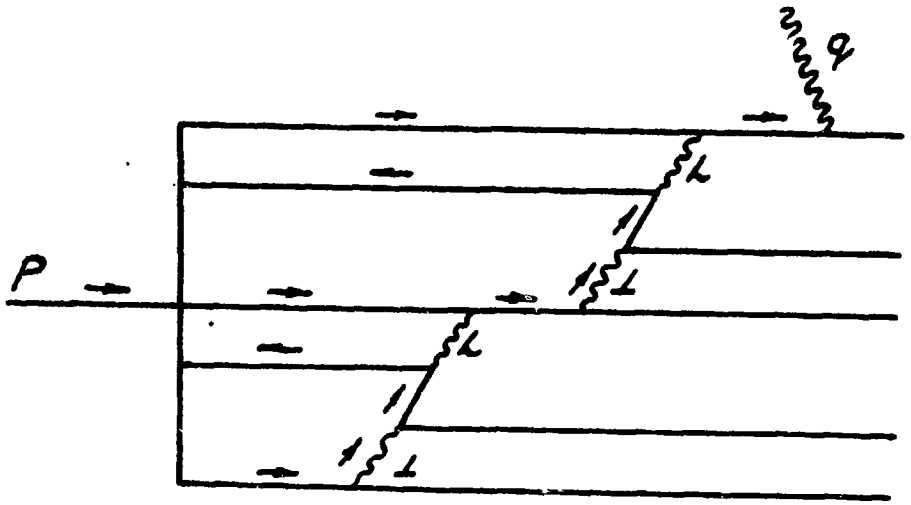

Fig.2

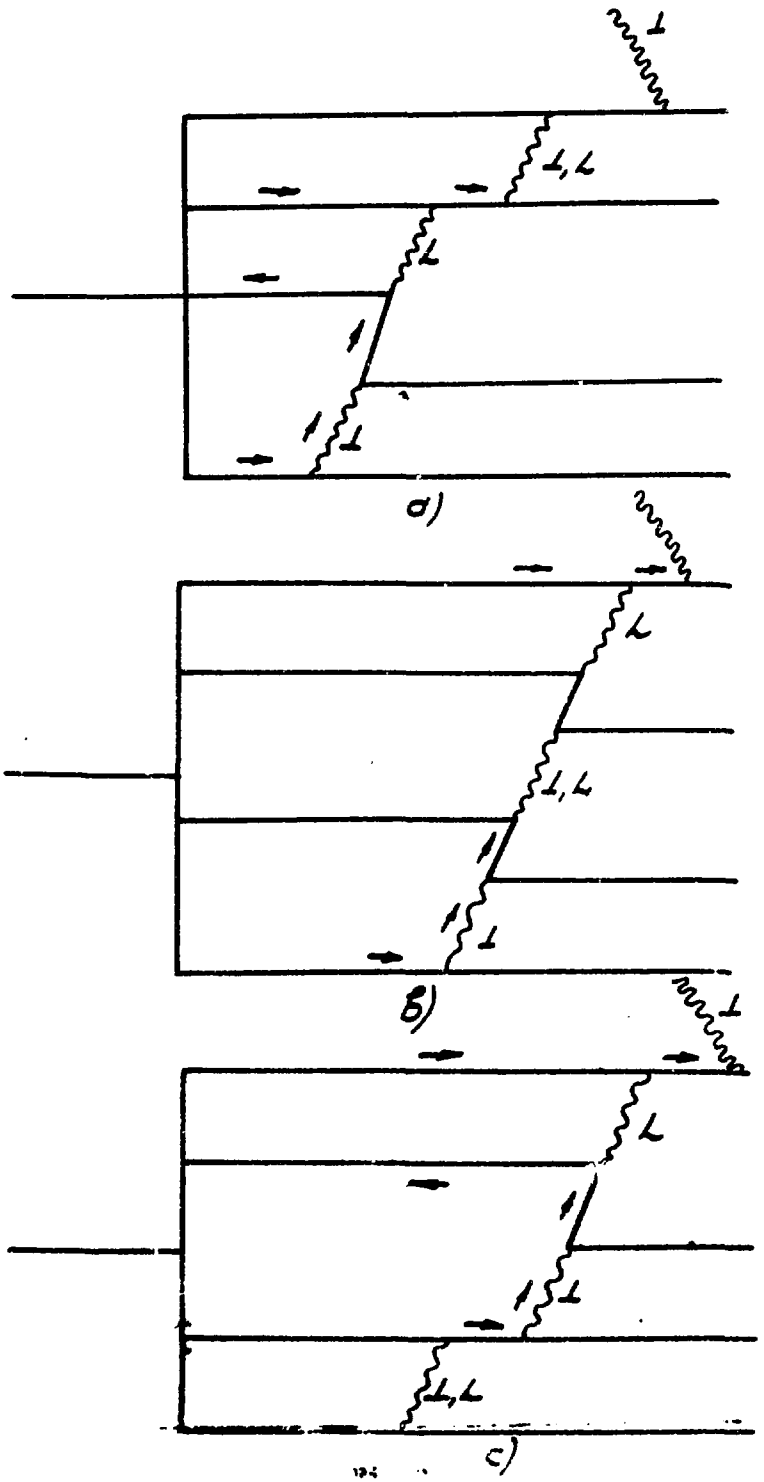
a)
b)
c)

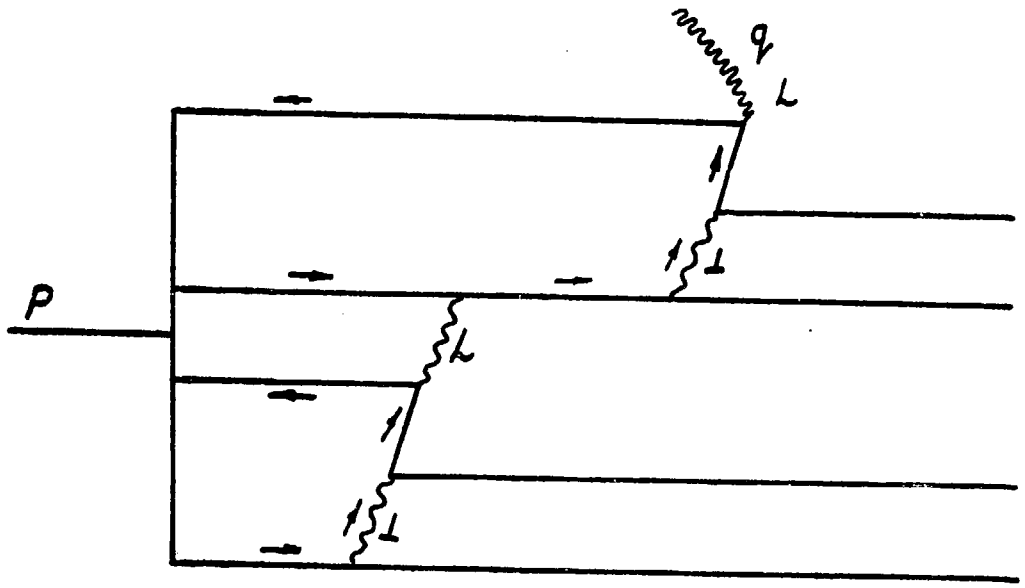

Fig.4

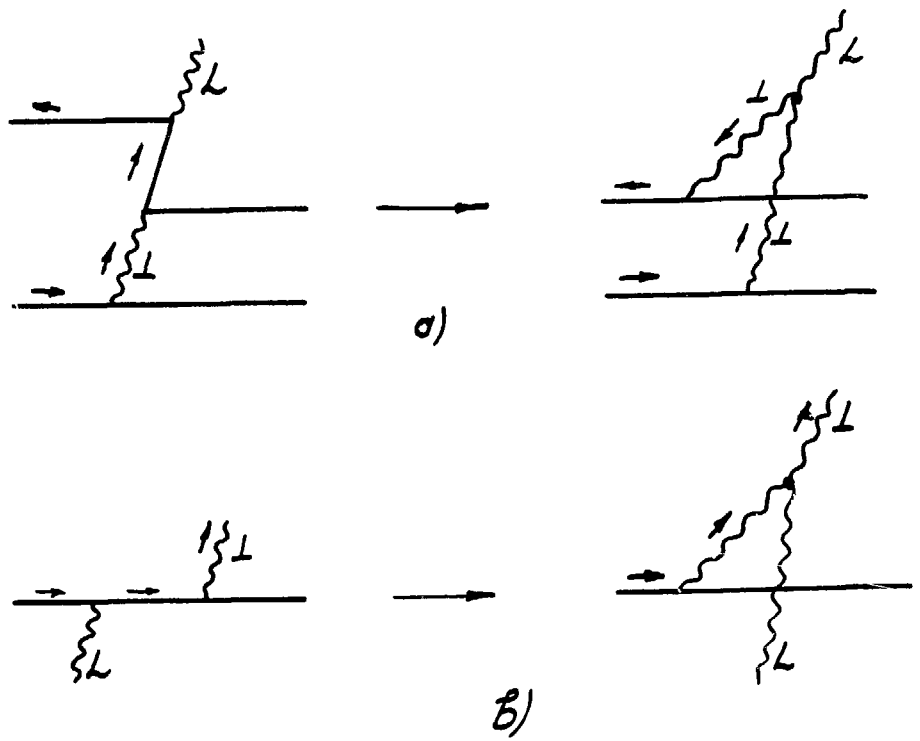

Fig.5

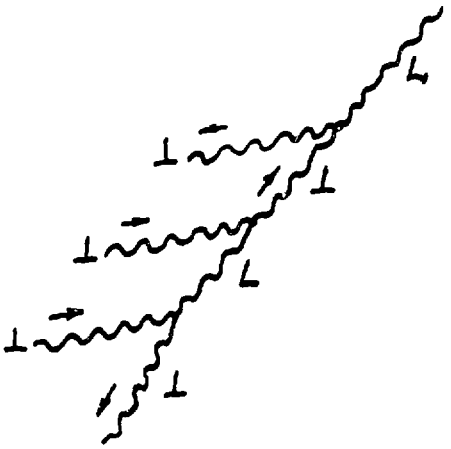

fig.6

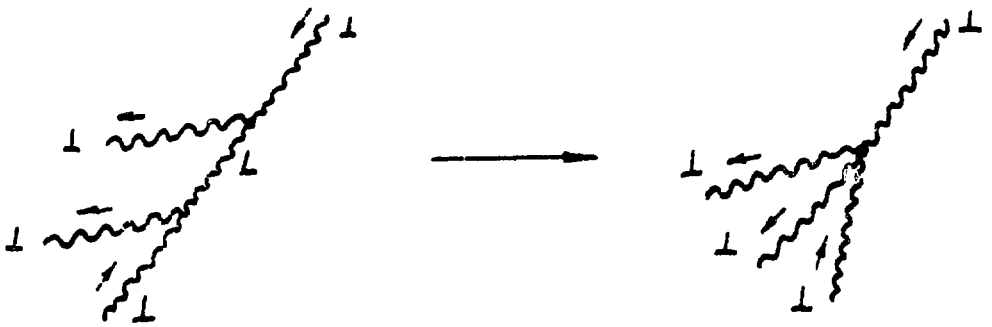

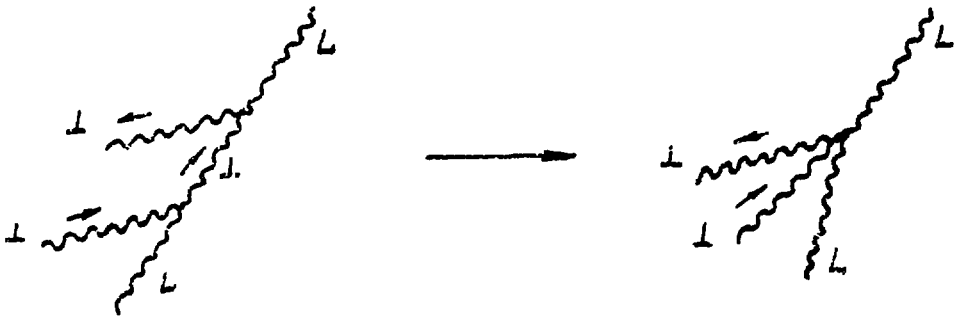

fig.7

Figure Capture

Fig. 1. The quark-gluon diagrams for the baryon structure function near x = 1

Fig.2. The dominant diagram for the n-quarks bound state's structure function near x = 1 for odd n.

Fig.3. The dominant diagram for the n - quark bound state's structure function near x = 1 for even n. The photon is transverse.

Fig.4. The dominant diagram for the n - quark bound states structure function near x = 1 for even n. The photon is longitudinal.

Fig.5. The replacements in the diagrams which lead to the accounting of the 3-gluon vertices.

Fig.6. The block of three-gluon verteces which appears after the replecements of Fig.5.

Fig.7. The replacements in the diagrams which lead to the accounting of the four-gluon verteces.

References

1. V.Matveev, R.Muradian, A.Tavkhelidze, Nuovo Cim.Lett. 7, 719 (1973); Brodsky, G.R.Farrar, Phys.Rev.Lett., 31, 1153 (1973); Phys.Rev. D11, 1309 (1975).
2. R.Blankenbeckler, S.Brodsky, Phys.Rev. D10, 2873 (1974); J.Gunion, Phys.Rev.D10, 242 (1974).
3. G.Morpurgo, Physics 2, 95 (1965).
4. E.M.Levin, V.M.Shekhter, Proc. of the 10th Winter School of LNPI on Nuclear Physics and Elementary Particles 1975, V.3.
5. D.J.Gross, F.Wilezek, Phys.Rev.Lett., 30, 1343 (1973); H.D.Politzer, Phys.Rev.Lett., 30, 1346 (1973).
6. G.R.Farrar, D.R.Jackson, Phys.Rev.Lett., 35, 1416 (1975)
7. M.B.Voloshin, L.B.Okun, Proc. of the 4th School of ITEP on Elementary Particle Physics, 1976, Vol.3, p.5.
8. S.J.Brodsky, B.T.Chertok, Phys.Rev. D14 , 3003 (1976)
9. D.J. Gross, F.Wilezek, Phys.Rev. D8, 3633 (1973).
10. R.Blakenbeckler et al. SLAC-PUB-1531 (1975)
11. S.D.Drell, J.M.Yang, Phys.Rev.Lett, 24, 181 (1970); G.West, Phys.Rev.Lett. 24, 1206 (1970).
12. R.P.Feynman, Photon-Hadron Interaction (Benjamin, 1972).
13. Bernard T.Feld, Models of Elementary Particles (Blaisdell 1969).
14. A.Smilda, "Yadrenaia Fizika", 25, 461 (1977)
15. P.V.Landshoff, DAMTP 76/73.
16. G.Grigoryan, S.B.Yesaybegyan, N.L.Ter-Isaakyan "Yadrenaia Fizika" 28.

The manuscript was received on the 22-th of July, 1977

С.Г.ГРИГОРЯН,С.В.ЕСАЙБЕГЯН,Н.Л.ТЕР-ИСААКЯН

О ПОВЕДЕНИИ СТРУКТУРНЫХ ФУНКЦИЙ АДРОНОВ ПРИ

$X \to I$

(на английском языке)

Ереванский физический институт

Тех.редактор А.С.Абрамян

Заказ 1146 ВФ-03394 Тираж 299

Подписано к печати 29/XI-77 Формат издания 30x40

I,8 уч.изд.л. Ц.12 к.

Издано Отделом научно-технической информации

Ереванского физического института,Ереван-36,пер.Маркаряна 2

индекс 3624